Long-time behavior of quasistationary states of the Hamiltonian mean-field model

Alessandro Campa
Complex Systems and Theoretical Physics Unit, Health and Technology Department, Istituto Superiore di Sanità and Istituto Nazionale di Fisica Nucleare, Sezione di Roma1, Gruppo Collegato Sanità, Viale Regina Elena 299, 00161 Roma, Italy

Andrea Giansanti and Gianluca Morelli
Physics Department, Università di Roma La Sapienza, Piazzale Aldo Moro 2, 00185 Roma, Italy

(Received 20 June 2007; revised manuscript received 7 August 2007; published 11 October 2007)

The Hamiltonian mean-field model has been investigated, since its introduction about a decade ago, to study the equilibrium and dynamical properties of long-range interacting systems. Here we study the long-time behavior of long-lived, out-of-equilibrium, quasistationary dynamical states, whose lifetime diverges in the thermodynamic limit. The nature of these states has been the object of a lively debate in the recent past. We introduce a numerical tool, based on the fluctuations of the phase of the instantaneous magnetization of the system. Using this tool, we study the quasistationary states that arise when the system is started from different classes of initial conditions, showing that the new observable can be exploited to compute the lifetime of these states. We also show that quasistationary states are present not only below, but also above the critical temperature of the second-order magnetic phase transition of the model. We find that at supercritical temperatures the lifetime is much larger than at subcritical temperatures.

DOI: 10.1103/PhysRevE.76.041117 PACS number(s): 05.20.−y, 05.10.−a, 05.70.Ln

I. INTRODUCTION

Many examples of long-range interacting systems can be found: self-gravitating systems [1], unscreened Coulomb systems [2], trapped charged particles [3], wave-particle interactions [4], vortices in two-dimensional fluid mechanics [5], magnets where dipolar effects are dominant [6]. The study of both equilibrium and out-of-equilibrium properties of systems with long-range interactions poses several challenges, that in recent years have been faced through analytical and numerical methods (for a review see, e.g., Ref. [7]). It has been shown that different statistical ensembles can be nonequivalent, so that the equilibrium states which can be reached by fixing certain thermodynamic parameters may be different from those obtained fixing other thermodynamic parameters. Rigorous results have been produced in this field [8]. The approach to equilibrium reveals the existence of transient states whose lifetime can diverge in the thermodynamic limit (i.e., when the number N of degrees of freedom of the system goes to infinity): these states can be called quasistationary states (QSS), and it is worth underlining that they are not metastable states, i.e., they are not stable local extrema of thermodynamic potentials, but their robustness is of dynamical origin [7]. Moreover, the characteristics of the QSS can depend on the initial conditions of the system. Another very interesting dynamical property is the breaking of ergodicity in microcanonical dynamics [9,10]. These facts imply that a deep understanding, in long-range systems, of kinetic effects, and in particular of the features of QSS, can be achieved considering both thermodynamics and dynamics and their intricate relationship.

This program has been pursued for several years on a simple model originally introduced in Ref. [11] and called the Hamiltonian mean-field (HMF) model. The model is an approximation of one-dimensional gravitational interactions, and it is also closely related to the Colson-Bonifacio model for free electron laser [12]. The Hamiltonian is

$$H = K + V = \frac{1}{2}\sum_{i=1}^{N} p_i^2 + \frac{1}{2N}\sum_{i,j=1}^{N} [1 - \cos(\theta_i - \theta_j)]. \qquad (1)$$

It refers to a system of N globally coupled rotators of unit mass, each one being described by the angle variable θ_i ($-\pi \leq \theta \leq \pi$) and by its conjugate momentum p_i (that in the following, for short, will be denoted as the velocity). The coupling constant is scaled by the number of rotators. This quite unphysical rescaling (the Kac prescription [13]) is necessary to ensure extensivity of the thermodynamic potentials, but it is not dramatic in the study of dynamical properties, since, as long as N is not infinite, it is equivalent to a rescaling of time.

The statistical mechanics of this system can be exactly solved, both in the canonical [11] and in the microcanonical [14] ensembles, that, for this model, have been shown to be equivalent. The system has a ferromagnetic second-order phase transition at a critical temperature $T_c = 0.5$, corresponding to a critical energy per particle (or energy density) $E_c/N = \epsilon_c = 0.75$. The magnetization, that spontaneously attains a nonzero value below the critical temperature, is the modulus M of the ensemble average of the vector

$$\mathbf{m} = (m_x, m_y) \equiv \frac{1}{N}\left(\sum_{i=1}^{N} \cos\,\theta_i, \sum_{i=1}^{N} \sin\,\theta_i\right), \qquad (2)$$

i.e., $M = |\mathbf{M}|$, with $\mathbf{M} = \langle \mathbf{m} \rangle$, is positive below the critical temperature. The lower bound for the energy density is $\epsilon = 0$.

Contrary to the equilibrium case, the out-of-equilibrium behavior of the system presents a great richness. This work aims at presenting some results concerning the dynamics of the HMF model. We describe the properties of the QSS that the system exhibits when the initial conditions belong to different classes. In the remainder of this section we give a

short summary of the results, connected with those presented in this work, that have already been obtained.

Microcanonical molecular dynamics simulations have shown that, for energy densities slightly below the critical value, QSS are present, whose lifetime diverges with a power of N. This implies that, if the thermodynamic limit $N\to\infty$ is performed before the infinite time limit, the system remains trapped in the QSS. While in the QSS, the distribution of the velocities p_i of the rotators is not Maxwellian [16]. The energy density that has been mostly considered is $\epsilon=0.69$; at equilibrium $M\approx 0.31$, corresponding to a temperature $T\approx 0.475$. In the simulations, the behavior of M is studied through the observation of the dynamical variable $m=|\mathbf{m}|$, while, as usual, the temperature is studied through the observation of the dynamical variable $2K/N$, i.e., 2 times the kinetic energy per particle (let us use, for this dynamical variable, the same symbol T of the thermodynamic temperature). It should be noted that the study of m in the microcanonical simulations is equivalent to that of T, since the conserved Hamiltonian (1) can be written as

$$H=\frac{N}{2}T+\frac{N}{2}(1-m^2). \tag{3}$$

The simulations have shown that the details of the dynamics in the QSS depend on the initial conditions. The most studied classes of initial conditions are those in which the initial value of m is either 0 or 1 (obtained with a uniform initial distribution of the θ_i or setting all θ_i equal to zero, respectively), while the velocities p_i are uniformly distributed in a range whose extension is determined by ϵ. When $m(0)=0$ it has been found that the lifetime of the QSS diverges as $N^{1.7}$ [15], while in the case $m(0)=1$ this divergence is linear in N [16]. In both cases the magnetization m in the QSS converges to zero for increasing N, although differences in the details of this convergence are observed. For example, starting with $m(0)=1$ the magnetization in the QSS, for a given N value, depends on the initial conditions (i.e., on the different realizations, for finite N, of the uniform velocities distribution, see Fig. 1); it is then necessary to perform several runs to obtain an average value. Starting from $m(0)=0$ the different runs are much more similar.

The observed non-Gaussian character of the velocity distributions has given rise to a lively debate on the characterization of these distributions. In particular, numerical investigations have concerned the tails of the distributions, to see if their decay is exponential (or even faster) [15], or if the decay could be fitted [17] to the expressions derived in the framework of nonextensive thermodynamics [18], that predicts tails decaying with a power law. The controversy has extended to the study of the anomalous diffusion [19,20], and fits to nonextensive thermodynamics expressions have been done also for the cases where the initial magnetization takes values between 0 and 1 and for the model where the coupling between rotators has a slow decay with distance [21] (see Ref. [22] for the generalization of the HMF model and a detailed study of its equilibrium behavior). In this paper we are not directly concerned with the characterization of the QSS in terms of ordinary Boltzmann-Gibbs (BG) or nonextensive thermodynamics, and we limit ourselves to the following remarks.

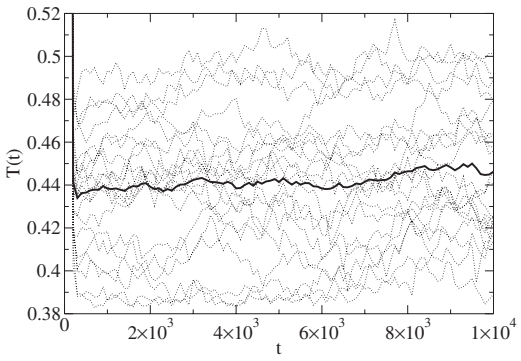

FIG. 1. Time evolution of temperature in the HMF model with $N=1000$, $\epsilon=0.69$, (wb) initial conditions. The full bold line is the average over 20 trajectories. The dotted lines refer to the individual trajectories that can considerably deviate from the average. Only considering a larger and larger number of rotators the fluctuations around the average tend to reduce.

Recent analytical calculations have shown that it is possible to interpret the QSS of the HMF model within a dynamical approach based on the Vlasov equation [15]. In fact, it has been proved [23] that, in the limit $N\to\infty$ the microscopic one-particle distribution function obeys this equation for a class of mean-field models, to which HMF belongs. Following the same line of research, it has then been argued that the QSS are formed in a short time through a fast relaxation to a state that maximizes an entropy functional of fermionic type [24,25], similarly to what happens for gravitational systems [26]. The approach to the QSS and its short-time behavior seems well reproduced by this theory, although some details need further explanations [25]. The long-time behavior, with the slow approach to the final BG equilibrium state, is much less understood from an analytical point of view, although again the Vlasov equation can be of help in justifying the very slow relaxation [15,19].

It is this long-time behavior that we are concerned with in this paper. We do not offer new analytical tools; rather, we study in details the characteristics of the velocity distribution functions of the QSS that arise when the dynamics starts from several different classes of initial conditions. The main point is the introduction of a new tool that characterizes the QSS, and that is based on the fluctuations of the phase of the magnetization. Mainly on the basis of this tool, we show that QSS are present also above the critical temperature, a fact that, up to now, has been overlooked in the literature.

In Sec. II we explain, referring also to Appendix A, the different classes of initial conditions. In the following three sections we present our results, focusing, respectively, on the role of the initial conditions on the properties of the QSS, on the dynamics of the magnetization using the new tool related to its phase, and on the QSS that occur at supercritical energy densities. The discussion, relating ours with previously presented results, follows in the last section.

II. NUMERICAL SIMULATIONS: THE DIFFERENT CLASSES OF INITIAL CONDITIONS

The equations of motion derived from Hamiltonian (1) can be written as

$$\ddot{\theta}_i = -m \sin(\theta_i - \phi), \tag{4}$$

where $m=|\mathbf{m}|$ and $\phi=\arctan(m_y/m_x)$ are the polar coordinates of the vector $\mathbf{m}$. The form of the equations clearly emphasizes the mean-field character of the system.

We underline that all our results concern microcanonical simulations, i.e., they refer to an isolated system. The equations of motion (4) have been numerically integrated with a fourth-order symplectic algorithm [27], with an integration time step $dt=0.1$, which ensures an energy conservation with a relative error of the order of 10^{-5}.

The initial conditions that have been explored in this work can be characterized by the one-particle distribution functions $f(\theta,p)$ that the initial values of θ_i and p_i are intended to realize. In this work we consider initial conditions in which the value m of the magnetization is initially 0 or 1, and a single case where it is 0.3. In all cases $f(\theta,p)$ is factorizable as $g(\theta)h(p)$. We refer to Appendix A for the expressions of the different distributions; here we limit ourselves to a few details. As $g(\theta)$ we always consider a distribution function that is constant inside a range and 0 outside; the range is determined by the value of m that one wants to set. For $h(p)$ we consider distributions with compact support (see Appendix A). Among the initial conditions here considered there are the two types that have been mostly used in the literature: (i) the so-called (wb) initial conditions, characterized by $g(\theta)=\delta(\theta)$ (i.e., $m=1$) and $h(p)=1/(2p_{\mathrm{wb}})$ between $-p_{\mathrm{wb}}$ and p_{wb}, with p_{wb} determined by the value of the energy, and (ii) the uniform (un) initial conditions, characterized by $g(\theta)=1/(2\pi)$ in the entire θ range (i.e., $m=0$) and $h(p)=1/(2p_{\mathrm{un}})$ between $-p_{\mathrm{un}}$ and p_{un}, with p_{un} again determined by the value of the energy.

III. THE ROLE OF THE INITIAL CONDITIONS IN THE OCCURRENCE AND IN THE PROPERTIES OF QUASISTATIONARY STATES

As mentioned in the Introduction, the microscopic one-particle distribution function $f(\theta,p,t)$ obeys, in the limit $N\to\infty$, the Vlasov equation [23]; in Appendix B we give this equation for the HMF system. For large values of N it is expected that the one-particle distribution will deviate from the solution of the Vlasov equation because of finite size effects, but these effects should be small. It is immediate to see that a distribution uniform in θ is a stationary solution of the equation; therefore, if in addition it is possible to prove its stability, one should expect that for large N such one-particle distribution will be maintained for a long time, giving rise to a QSS. Uniformity in θ is not a necessary condition for stable stationarity with respect to the Vlasov equation, therefore, it is possible to find also nonuniform distributions that produce a QSS. The two questions related to this fact are the following: (i) if the system is prepared in a generic initial condition, i.e., a state that is not a stable stationary solution of the Vlasov equation, one would like to know if it reaches such a state, and thus remains in a QSS before eventually going to BG equilibrium; (ii) when the system is in a QSS, either by preparation or by reaching it from a generic initial condition, what are the modalities by which the system reaches BG equilibrium, and how the modalities depend on the preparation of the system. The first question has been recently studied [24,25] for a simple particular class of initial conditions, that should relax in a short time to a QSS; answers to the second questions up to now are only of numerical nature, relying on results of simulations, with the exceptions of some arguments again based on the Vlasov equation [15,19]. The QSS lasts for a time proportional to a power of N, after which the one-particle distribution relaxes to the BG equilibrium expression

$$f(\theta,p) = A^{-1} \exp\left(-\frac{\beta}{2}p^2 + \beta M \cos(\theta-\phi)\right), \tag{5}$$

where the values of the inverse temperature β and of the spontaneous magnetization M are those computed in the microcanonical or canonical ensembles, and where the normalization factor A is proportional to $I_0(\beta M)$, the modified Bessel function of order 0. When $M\neq 0$, the magnetization phase ϕ is determined by the boundary conditions. It is useful to stress again that the QSS are not thermodynamical metastable states, and therefore their properties cannot be deduced by the study of thermodynamical potentials. In this paper we provide more extended numerical results on the relaxation to equilibrium of QSS, especially with the introduction of new tools.

If the dynamics of the system starts from random $\theta_i(0)$ and $p_i(0)$, it usually does not get trapped into a QSS, so that the one-particle distribution function rapidly reaches the form (5), then the temperature and average magnetization attain their BG values. Only the preparation in selected nonequilibrium initial conditions induces a dynamics that generates a QSS. This is plausible, especially on the basis of point (i) treated above: apart from the case in which the system is prepared in a stable stationary solution of the Vlasov equation, it is not expected that the rapid early evolution of a generic initial evolution will lead to such a solution.

Usually, the QSS have been studied at energy densities ϵ slightly below the critical value 0.75, and mostly at the value 0.69. However, it seems that there is no argument that prevents QSS from occurring also above the critical value 0.75. In fact, in this work we observe that QSS exist even at supercritical energy densities.

A. Water bag initial conditions

In the (wb) initial conditions, as put in evidence in the corresponding distributions in Appendix A, the initial angles are all set to zero and the initial velocities are sampled from a uniform distribution centered on zero; the initial configuration has magnetization $m=1$, and therefore $T=2\epsilon$, as can be seen from Eq. (3). Simulations at energy densities in the range between 0.68 and 0.75 have shown that the temperature falls onto a nonequilibrium plateau value T_{qss} within a

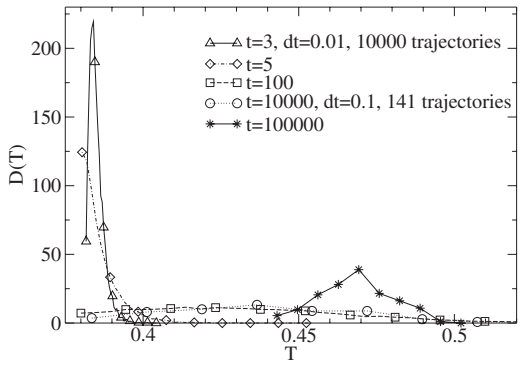

FIG. 2. Dispersion of the temperature around the average in the HMF model, (wb) initial conditions. Data refer to the case of $N=1024$ rotators, $\epsilon=0.69$; each dot is an average over 100 time steps. Note that, for this number of rotators, after the spread from the initial value (curves corresponding to $t=3$ and $t=5$), temperatures fall in a large interval up to times 10 000 (approximately, the lifetime of the quasistationary state). Only over time 100 000, when the system relaxes toward equilibrium, they tend to concentrate around the equilibrium value of 0.475, expected for the energy density here considered. Short trajectories have been simulated with a smaller time step, as indicated.

few time steps [16]. However, the N-dependent value of T_{qss} is an average over many trajectories, i.e., over many realization of the (wb) initial conditions. For example, if $\epsilon=0.69$, the statistical mechanics solution of the model gives an equilibrium temperature $T_{\mathrm{eq}}=0.475$, while $T_{\mathrm{qss}}<T_{\mathrm{eq}}$. Correspondingly [see Eq. (3)], the initial unitary magnetization gets very rapidly a small value, close to zero, that characterizes the QSS, and, after a time diverging with N, reaches the equilibrium value $M=0.31$. A characteristic of the (wb) initial conditions is the presence of large sample-to-sample fluctuations in the relevant observables (temperature and magnetization). Figures 1–3 illustrate this intrinsic randomness in the typical case of $\epsilon=0.69$: Figure 1 shows the temperature time course for 20 different trajectories with $N=1000$, together with the average time course; Fig. 2 plots the dispersion, at different times, of the temperature: the dispersion shrinks only when the system relaxes to BG equilibrium. Fluctuations around the average temperature of the QSS decrease with increasing N; in addition, when N increases, the average temperature of the QSS decreases and tends to the value 0.38, corresponding, according to Eq. (3), to zero magnetization. Figure 3 puts in evidence the decrease of the average QSS temperature when N is increased, and it shows, for the largest N value, the time fluctuation of the QSS temperature of a single trajectory. In Ref. [28] one can find a study of the dependence of the average QSS temperature as a function of the initial magnetization m.

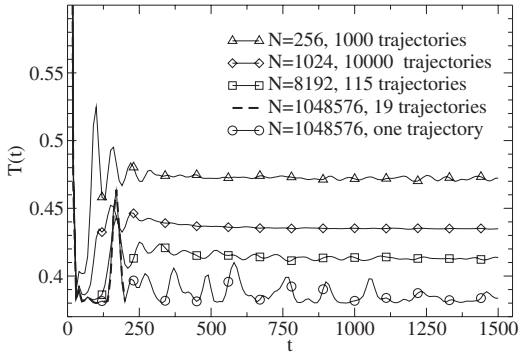

FIG. 3. Time evolution of the average temperature as a function of N, in the HMF model, for the (wb) initial conditions. Note that increasing the number of rotators the temperature of the quasistationary state tends to the value of 0.38, corresponding to a zero magnetization state with energy density $\epsilon=0.69$.

B. Other classes of initial conditions and the attracting velocity distribution function

The (wb) initial conditions are implemented with a random extraction of the initial velocities from a uniform distribution centered around zero. However, it is possible to assign deterministically the initial velocities with the prescription $p_i=-p_{\mathrm{wb}}+2p_{\mathrm{wb}}(i-1/2)/N$, $i=1,2,\ldots,N$, with p_{wb} defined in Appendix A as a function of the energy density ϵ. We have called this special initial condition (iwb) (they had been independently introduced in Ref. [29]). For $N\to\infty$ any realization of the (wb) should not differ appreciably from the (iwb). We have found that this particular realization of the water bag conditions does not produce time fluctuations of the dynamical temperature. Moreover, in this case, the QSS temperatures do not depend on N and are very close to the large N value of the average QSS temperature observed in the case of the mostly used (wb) initial conditions [30].

Besides the absence of fluctuations, it is remarkable that, at variance with the (wb), the QSS arising from the (iwb) initial conditions behave very similarly to those produced by the two classes of initial conditions that we have studied, in which the initial magnetization m is set equal to zero. In fact, the (iwb), the (un), and (tr) initial conditions all share the following properties: (i) the magnetization in the QSS is given, as a function of N, by $m\simeq 2N^{-1/2}$ (thus it is asymptotically zero for large N), and, consequently, $T\simeq 2\epsilon-1+4/N$; (ii) the initial velocity distribution evolves in a short time toward an attracting distribution, whose shape is approximately a semiellipse (see Fig. 4).

The velocity distribution function becomes Maxwellian when eventually the system goes to BG equilibrium, leaving the QSS. Following this observation, one could represent the function $h(p)$, during the QSS, exactly with a semiellipse (that will therefore be equal to the elliptical (el) initial conditions described in Appendix A). The two parameters (i.e., the semiaxes of the ellipse) are fixed by the energy density and by the normalization condition, and the shape is fixed. It is not surprising that, as we show in Appendix B, at $\epsilon=0.69$ the elliptic velocity distribution function satisfies the condition for its stability as a stationary solution of the Vlasov equation [15,31], if $\epsilon\geq 0.625$. In Ref. [15] a similar attracting distribution was found, although it was not parametrized as an ellipse and its Vlasov stability through Eq. (B3) was not studied. It should be remarked that the velocity distribution function evolves in time. Nevertheless, during the QSS, the evolution is very slow, and the elliptical represen-

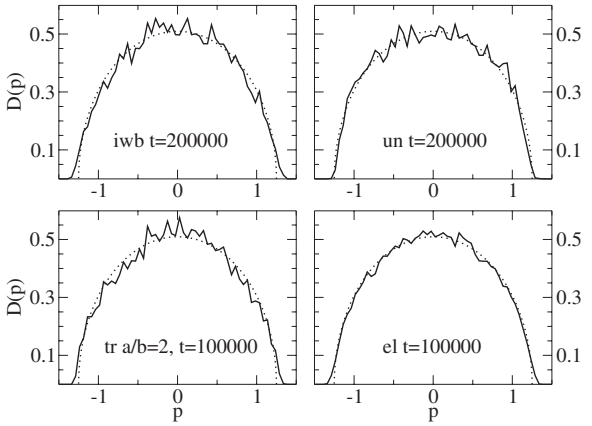

FIG. 4. Long-time velocity distribution function (full lines) for different initial conditions (see Appendix A for the meaning of the acronyms). In this case $N=16\,384$, $\epsilon=0.69$. For the (tr) initial conditions we give the ratio of the distribution parameters. The same fitting semielliptical distribution is shown in each plot with dotted lines.

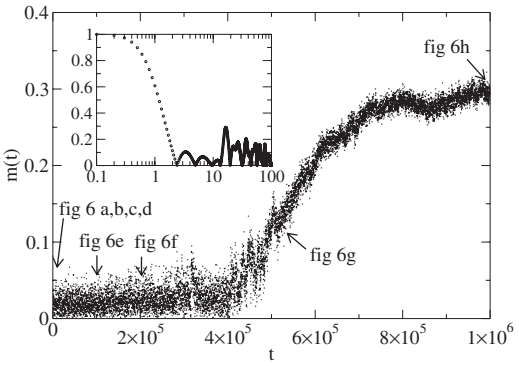

FIG. 5. Time evolution of the modulus of magnetization of the HMF model, (iwb) initial conditions. Note that for this class of initial conditions the initial magnetization abruptly falls on a very small value plateau, which tends to zero, increasing N, approximately as $N^{-1/2}$. A null magnetization is associated to the quasistationary state. In the inset: details of the short-time behavior. Data refer to the case: $N=10\,000$, $dt=0.1$, $\epsilon=0.69$. For this number of rotators the lifetime of the quasistationary state is around 4×10^5, then there is a transient ending around 7×10^5, then the equilibrium value for the actual value of the energy density is reached, $|\mathbf{M}|=0.31$. The arrows indicate times at which snapshots of the μ space are shown in the corresponding panels of Fig. 6.

tation will remain a good approximation until the relaxation toward BG equilibrium starts, when tails in the distribution begin to develop.

It is then clear that, if the elliptical velocity distribution is chosen as the initial condition [the (el) initial conditions of Appendix A], the system will be prepared in a slowly evolving QSS, without any initial transient characterized by a shorter time scale.

In the following section we show, in particular, the occurrence of the QSS with elliptical velocity distribution function when the dynamics starts from the (iwb) initial conditions. We then study the lifetime of this QSS as a function of N, introducing a new determination of this dependence on the basis of the fluctuations of the phase of the magnetization. Furthermore, we will show that QSS are present also at supercritical energy densities.

IV. THE DYNAMICS OF THE MODULUS AND OF THE PHASE OF THE MAGNETIZATION

A. Relaxation dynamics of the magnetization and parallel evolution of the velocity distribution

In this section we follow the time evolution of the modulus of the magnetization, in parallel with the evolution of the one-particle distribution function $f(\theta,p)$ and of its integral over the positions, i.e., the velocity distribution function. This is done for the (iwb) initial conditions at $\epsilon=0.69$, with $N=10\,000$. As we pointed out, in this case the equilibrium magnetization is equal to 0.31.

We show in Fig. 5 the dynamics up to time 10^6. The quasistationary state is characterized by a small value of the magnetization around 0.02, that persists until times of about 4×10^5, when the relaxation toward equilibrium starts. As shown in the inset of Fig. 5 the magnetization modulus, initially equal to 1, falls to small values in $O(1)$ time, with some bounces before setting to the above-mentioned value of about 0.02. The arrows in Fig. 5 denote the times at which the snapshots shown in Fig. 6 are taken. This figure shows the evolution of the one-particle distribution function $f(\theta,p)$ and of the velocity distribution function. The first one is represented plotting on the (θ,p) plane the canonical coordinates of all the rotators. One can see that during most of the duration of the QSS, namely, from a time of about 10^4 up to the time when relaxation to BG equilibrium begins, around 4×10^5, the velocity distribution function is characterized by the elliptical shape, illustrated in Fig. 4. The QSS ends when the semielliptical distribution starts to develop tails and eventually becomes a Maxwellian. Correspondingly, the developing finite magnetization can be spotted in the dishomogeneous appearance of the left-hand plot of panel (h) of Fig. 6.

When the dynamics starts with the unified (un), (tr), and (el) initial conditions, the evolution of the velocity distribution functions is practically the same as that presented in Fig. 6 [in the last (el) case there is not even an initial transient]. In these cases the magnetization m is practically 0 from the beginning.

The previous results indicate that the QSS arising from these four classes of initial conditions can be described by an almost-zero magnetization state, characterized by a semielliptical velocity distribution function. In the next section the QSS is further characterized by a new quantity, the angular frequency of the magnetization, determined by the dynamics of the argument of the magnetization.

B. Quasistationary states and angular frequency of the magnetization

In the QSS the argument ϕ of the (very small in modulus) magnetization displays a strongly fluctuating behavior, cor-

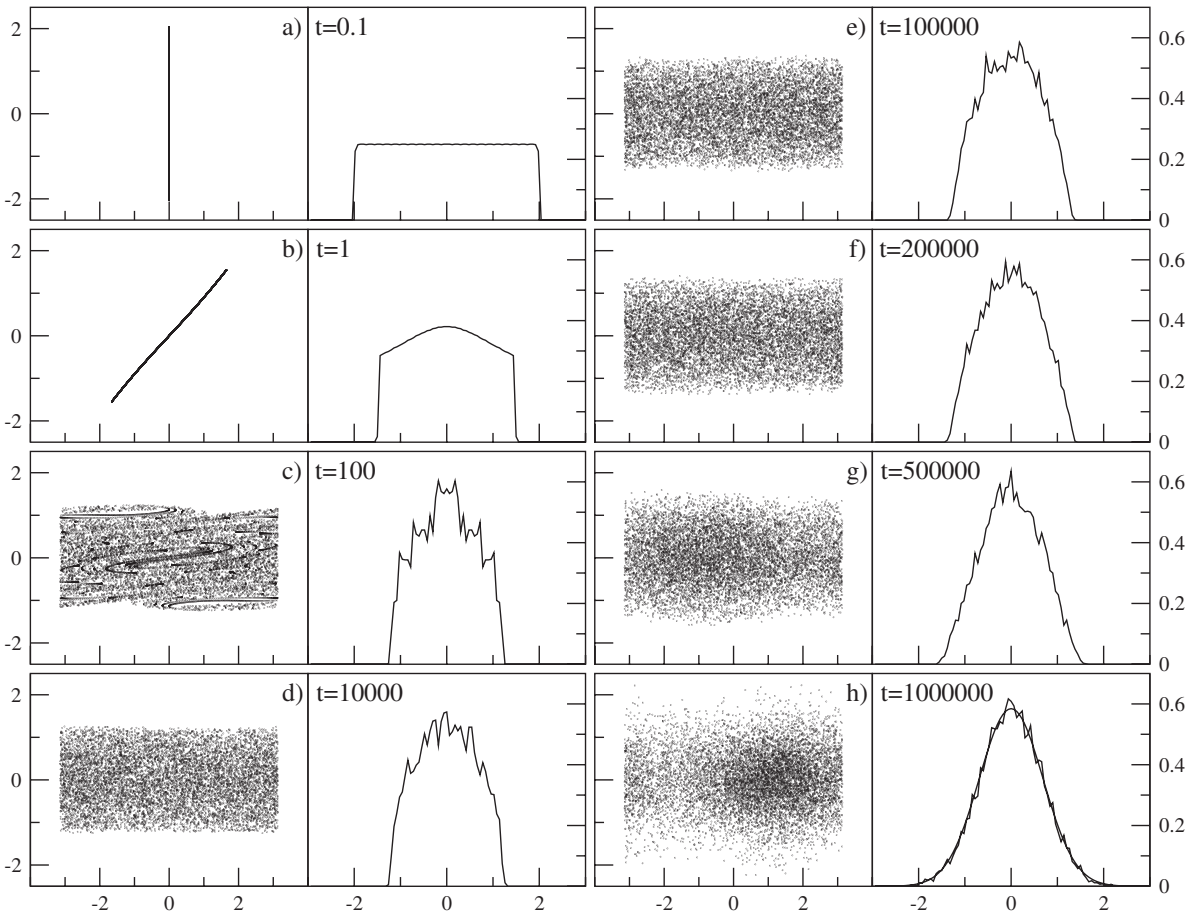

FIG. 6. Time evolution of the μ space and, in parallel, of the distribution of velocities, (iwb) initial conditions. The run is the same as that reported in Fig. 5: $N=10\,000$, $dt=0.1$, $\epsilon=0.69$, where the corresponding times are marked by arrows. Clearly, after a very short initial time the velocity distribution reaches a shape that is easily fitted to an elliptic profile. The elliptic distribution is maintained until the dynamics is in the quasistationary state. After, approximately, $t=4\times10^5$ the distribution starts to develop tails and, after a transient, it becomes evidently Gaussian, in the equilibrium state. Data in panel (h) have been fitted to the Maxwellian, $y=C\exp[-(x^2/2T)]$, the fitted temperature result is 0.475, as expected.

responding to frequent and abrupt changes in direction. During the relaxation toward equilibrium, while the modulus increases toward its equilibrium value, the fluctuations are much less violent. This different behavior is plausible, considering the large ratio between the modulus of the equilibrium magnetization and that of the QSS magnetization. We found that this difference can be exploited to give a convenient characterization of the QSS. In particular, indicating with dt the integration time step, we define the following cumulative quantity:

$$\sigma_m(t) = \sum_{n=0}^{t/dt} |\arg\{\mathbf{m}[(n+1)dt]\} - \arg[\mathbf{m}(ndt)]|. \qquad (6)$$

This is the sum of the absolute values of the angular distances spanned by the magnetization vector during an integration time dt, sampled up to time t. Let us note that this observable is monotonically increasing with t, but it is also time-step dependent: for given t, it is monotonically not decreasing if the sampling interval dt is decreased. Figure 7, that shows both the modulus $m(t)$ and the quantity $\sigma_m(t)$, refers to a typical trajectory started from the (el) initial conditions, i.e., directly from the QSS. From the plot it is evident that there is a crossover between two regimes, passing

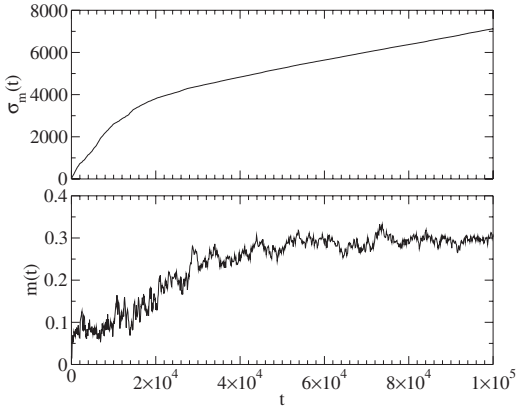

FIG. 7. Time evolution of the function $\sigma_m(t)$ and of the modulus of the magnetization, (el) initial conditions. Data refer to the case $N=1024$, $\epsilon=0.69$.

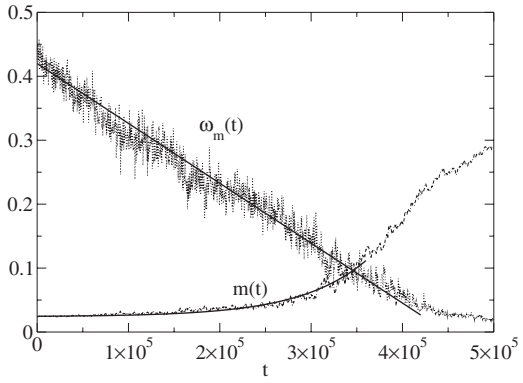

FIG. 8. Time evolution of magnetization and of the angular frequency in a typical case: $N=8192$, $\epsilon=0.69$, (el) initial conditions, average over 10 trajectories.

from the QSS to the BG equilibrium state. The crossover is characterized by the change in the derivative $\omega_m(t)$ of $\sigma_m(t)$. We find that it is possible to fit the observed time evolution of $\sigma_m(t)$ with

$$\sigma_m(t) = \omega_{m,\mathrm{qs}} t - Ct^2 \tag{7}$$

in the QSS, and with

$$\sigma_m(t) = \omega_{m,\mathrm{eq}} t \tag{8}$$

in the equilibrium state. Therefore,

$$\omega_m(t) = \omega_{m,\mathrm{qs}} - 2Ct \tag{9}$$

in the QSS, and

$$\omega_m(t) = \omega_{m,\mathrm{eq}} \tag{10}$$

in the equilibrium state. We found that $\omega_{m,\mathrm{qs}}$, the derivative in zero of $\sigma_m(t)$, depends on the energy density, but appears to be independent of the system size N; on the contrary $\omega_{m,\mathrm{eq}}$ decreases as N increases, going as the inverse square root of N, while C depends both on N and the energy density. Namely, it increases with ϵ and decreases with N. In Fig. 8 we show both $m(t)$ and $\omega_m(t)$ for a given N value at $\epsilon=0.69$, while in the left-hand panel of Fig. 9 we plot, for the same energy density, the behavior of $\omega_m(t)$ for different values of N. In all cases we start from (el) initial conditions. According to Eqs. (9) and (10), and as Figs. 8 and 9 show, $\omega_m(t)$ linearly decreases with time in the QSS, and then tends to level off, when the system reaches the equilibrium state. From the left-hand panel of Fig. 9 it is also possible to see the mentioned independence on N of $\omega_{m,\mathrm{qs}}$, while the different slopes prove the marked dependency on N of C in Eq. (9).

The change of behavior implicit in the passage from Eq. (9) to Eq. (10) seems to be much more clear cut than the gradual increase of the magnetization (or of the temperature) at the start of the relaxation to equilibrium. Therefore, the time evolution of $\omega_m(t)$ can be used to define the lifetime of the QSS in an easier way. In fact, let us define this lifetime by the time in which the linear fit of $\omega_m(t)$ in the QSS extrapolates to zero. Because of the independence on N of $\omega_{m,\mathrm{qs}}$, this intercept is inversely proportional to C. The right-hand panel of Fig. 9 plots the dependence of C on N, and from this plot it is possible to reconstruct the scaling law of the QSS lifetime. Values of $C(N)$ have been obtained for several trajectories for each N, and in the plot we give average values with standard deviation error bars. From the fitting line we can evaluate the scaling exponent of the dependence on N of $C(N)$. The QSS lifetime, as we have just defined it, is inversely proportional to C, and therefore its scaling exponent with N is just the opposite of that of $C(N)$. We obtain the value 1.7 ± 0.1, in agreement with previous determinations. Similar graphs are obtained for the other classes of initial conditions that rapidly evolve to the semielliptical distribution.

The angular frequency of the magnetization, introduced here, provides a very convenient operational definition of the QSS. The latter have been searched for, until now, exclusively at subcritical energy densities, i.e., for $\epsilon\leq0.75$. However, the observations presented in the next section, based on the quantities just introduced, indicate that QSS can be present also at supercritical energy densities.

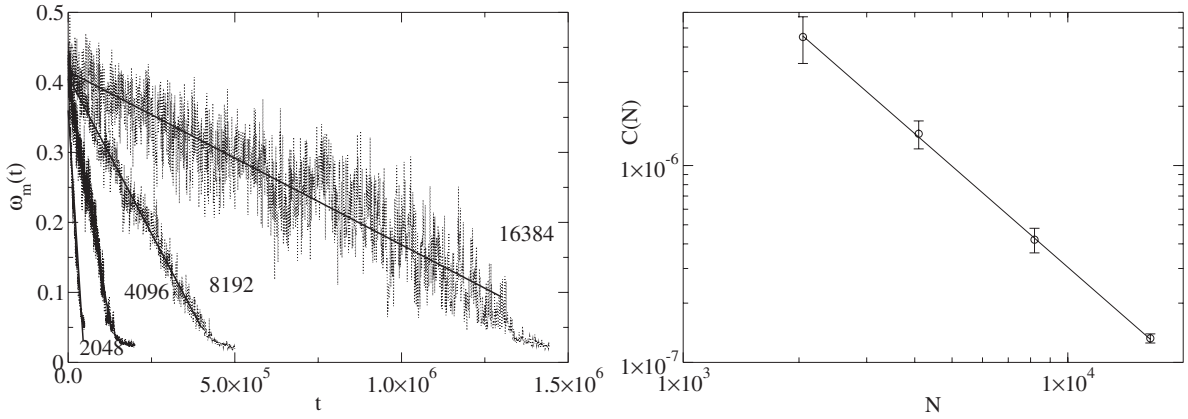

FIG. 9. Left-hand panel, time evolution of angular frequency of magnetization: N dependence, $\epsilon=0.69$, (el) initial conditions. Right-hand panel, dependence on N of the parameter C. Error bars represent standard deviations. The power-law dependence on N of the QSS lifetime can be estimated from the slope of the linear regression of $C(N)$. The fitted exponent of $C(N)$ is -1.7 ± 0.1.

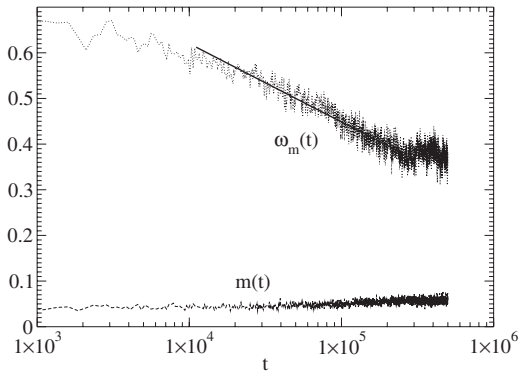

FIG. 10. Time evolution of the magnetization and of the angular frequency of magnetization in the supercritical case: $N=1024$, $\epsilon=0.8$, (el) initial conditions, average over 20 trajectories.

V. SUPERCRITICAL QUASISTATIONARY STATES OF THE HMF

The behavior of $\omega_m(t)$ shows that, by starting from the (el) initial conditions, the system can be set in a QSS even at supercritical energy densities. In Fig. 10 we show the time evolution of $\omega_m(t)$ and that of $m(t)$ at the supercritical energy density $\epsilon=0.8$. Note that, also in this case, it is possible to distinguish two regimes. The crossover is around the time 2×10^5. Now $\omega_m(t)$ crossovers from a logarithmic decay with time to a constant, when the system relaxes to BG equilibrium. In this supercritical case the equilibrium value of the magnetization is zero and the relaxation to equilibrium is characterized by the velocity distribution function that becomes Maxwellian; this happens at the crossover of $\omega_m(t)$, as we have checked. Although at the crossover the magnetization modulus should remain very small, in Fig. 10 there is trace of a small relaxation, possible signature of a finite size effect.

In Fig. 11 we show that the slope of $\omega_m(t)$ in the QSS is substantially independent of system size, but the function is multiplied by an N-dependent factor, as indicated by the parallel translation of the signal. This is the opposite behavior with respect to the subcritical case. In addition, note the

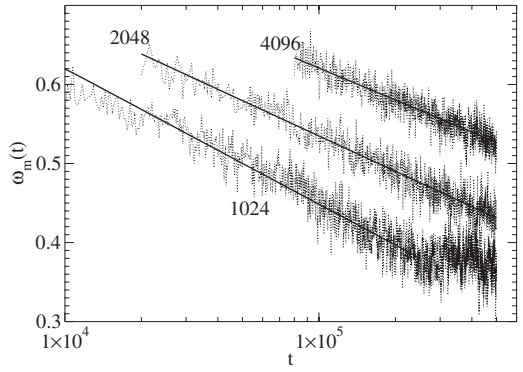

FIG. 11. Supercritical case. N dependence of the time evolution of the angular frequency of magnetization. $\epsilon=0.8$; in each case average over 20 trajectories.

logarithmic time axis, that points, in the supercritical case, to an exponential increase of the QSS lifetime with the system size.

VI. DISCUSSION

We would like to begin this section with some comments on the relation of the QSS in the HMF model with the results that have been obtained for self-gravitating systems. The confinement of these systems makes it possible to have local extrema of the thermodynamic potential, entropy or free energy, depending on the ensemble under consideration, microcanonical or canonical; this implies the existence of metastable states (see, e.g., Refs. [32,33]). The lifetime of these metastable states is proportional to the exponential of the thermodynamic potential barrier that separates them from the global extremum [34]; this barrier in turn is proportional to the number of degrees of freedom, i.e., to the system size. This is analogous to what has been found for metastable states in simple magnetic systems [10,35]. We have already emphasized that the QSS of the HMF model are not metastable states, since they do not correspond to local extrema of the thermodynamic potential, and their robustness is of dynamical origin. However, it is still possible to argue a connection with some results concerning confined self-gravitating systems. In fact, it has been found that collapse and explosion in these systems (the two processes describing the transition, respectively, between the uniform and core-halo structure and vice versa) can be extremely slow, their duration being proportional to the exponential of the frequency ratio between fast and slow modes [36,37]. These transitions are considered in the cases where the state, from which the system departs, has lost its (meta)stability character, and therefore the situation is closer to the QSS of the HMF model. Details are obviously different, due to the very different nature of the systems: in the collapse of the self-gravitating system it is not the formation of core and halo structures that takes the longest time, but rather the exchange of energy between core and halo particles, to reach equilibration. In the HMF model it seems that the formation of the magnetized configuration, required by BG equilibrium, is attained only in the final stages of the QSS, at the same time of the final equilibration of the velocities in a Maxwellian distribution. Below we comment on how finite size effects are responsible for the approach to BG equilibrium, when we look at the HMF model in the framework of the Vlasov equation. However, looking from another point of view, it would be interesting to see if slow energy exchanges between fast and slow modes are the main cause of the long lifetime of QSS, analogously to the mentioned transition in self-gravitating systems, in spite of the cited differences.

In this paper we have considered different classes of initial conditions. We have observed that at long times, before the relaxation to equilibrium, for the classes of initial conditions with $m(0)=0$ and for the (iwb) initial conditions, which have $m(0)=1$, the velocity distribution function acquires an elliptical shape; this is shown in Fig. 4. This special functional form is a stable solution of the Vlasov equation, as shown in the Appendix B and in Fig. 13. These results are

consistent with the attracting character of the elliptic velocity distribution function.

The quasistationary states of the HMF have been phenomenologically characterized through the dynamics of both the magnetization modulus and phase. These states are characterized by the small value, $O(N^{-1/2})$, of the magnetization modulus and by a linear decay in time of the angular frequency of the magnetization, an observable used here for the first time, that has been very useful to revisit the power-law behavior of the QSS lifetimes as a function of N. Moreover, this observable was effective in showing that long-lasting dynamical states, quite similar to the subcritical QSS, are present also at supercritical energy densities; it has been shown that in this case the time scale for the approach to BG equilibrium is much greater.

Recent work on the short-time behavior of the HMF model [25] has studied the dynamics on the basis of an entropy functional which is suitable for systems in the collisionless approximation [26], which is generally valid for mean-field systems, and where the dynamics satisfies the Vlasov equation. Actually, the study was restricted to the cases where the initial one-particle distribution function has only two values: a constant in a given region of the one-particle phase space, and zero outside (i.e., the authors consider only uniform initial distribution functions, realizing different initial magnetizations). The dynamical mixing in the one-particle phase space will lead, in a short-time scale (fast relaxation), to a QSS, characterized by a one-particle distribution function that is a stable stationary solution of the Vlasov equation, and that maximizes the entropy functional; the particular shape of this distribution function depends on the initial magnetization [38]. Numerical simulations, limited to very short times, were performed for comparison with the analytical calculation: these show that, at the energy density $\epsilon=0.69$, the QSS has a zero magnetization, unless the initial value $m(0)$ is above a critical value around 0.9 [25]. Finite size effects, acting as a perturbation term in the Vlasov equation, will then be responsible, at large times, of the approach to the BG equilibrium. Our uniform initial distribution function, with $m(0)=0$, belongs to the class studied in Ref. [25]. In this particular case the initial distribution is already the stable stationary solution maximizing the entropy functional, and there should be no fast relaxation. This seems to contradict our numerical results, obtained also in Ref. [15], showing that, when we start from the (un) initial conditions, the distribution function has a semielliptical shape while the system is in the QSS. Then, to have another comparison, we have investigated also a case with initial magnetization between zero and one. The corresponding uniform initial distribution is the one called partial magnetized (pm) in Appendix A. We have considered the case $m(0)=0.3$, and Fig. 12 shows the distribution at different times. In this case we find that, during the QSS, the distribution function maintains the shape reached after the first fast relaxation, that in turns agrees with that obtained in Ref. [25]. The different behavior between the (un) and the (pm) initial conditions can therefore be summarized in the following. The dynamics starting from the (pm) conditions has a fast relaxation toward a QSS, with the velocity distribution slowly evolving, afterwards, to the BG equilibrium form. Starting from the corresponding uniform (un) conditions, where fast relaxation does not take place, the velocity distribution has nevertheless an evolution toward the elliptical form, although quite slower than the fast relaxation; from there, the distribution slowly evolves toward BG equilibrium.

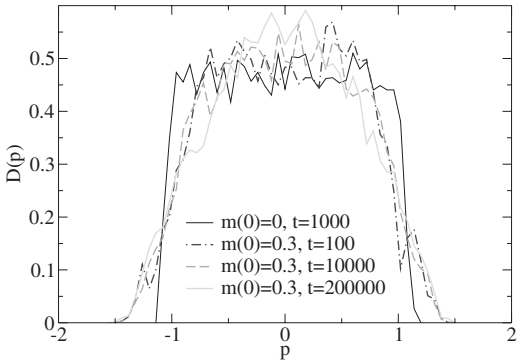

FIG. 12. Velocity distribution function at long times. The initial magnetization has been set to $m(0)=0.3$; $N=10\,000$, $\epsilon=0.69$.

One can argue that a possible explanation of these different behaviors can be ascribed to a different influence of finite size effects on both cases, according to the following.

As noted before, once in the QSS, the velocity distribution evolves very slowly, passing through a series of stable stationary states of the Vlasov equation [15]. Finite size effects are responsible for this very slow dynamics. As we have checked numerically, when this slow evolution drives the velocity distribution to a situation where the stability condition (Appendix B) is no more satisfied, a faster approach to BG equilibrium takes place. However, finite size effects are present also during the initial dynamics. They have been studied in Ref. [39], again on the basis of the Vlasov equation, but without any reference to entropy functional; i.e., through a purely dynamical approach. It has been shown that the one-particle distribution function is modified by a diffusion process. The corresponding diffusion coefficient is proportional to $1/N$, but the proportionality coefficient can be extremely large for the (un) initial distribution function. This would tend to modify the distribution function rapidly. It would be interesting to perform the same calculation in the case of the elliptic function, to have a confirmation that in this case the proportionality coefficient is much smaller.

The classes of initial conditions considered in this work all share the property that the initial velocity distribution does not have tails, being with compact support. This seems to be a requisite for the formation of QSS, at least for the cases in which the initial angle distribution is uniform; in particular, initial conditions at subcritical energy, e.g., $\epsilon=0.69$, in which the angles are uniformly distributed, i.e., $m(0)=0$, and the velocities are distributed according to a Maxwellian, with an out-of-equilibrium temperature, relaxing rapidly toward BG equilibrium. This numerical result is supported by the stability analysis described in Appendix B applied to this situation, that shows that the Maxwellian velocity distribution function, associated to a uniform angle distribution, does not satisfy the stability condition if the

energy ϵ is below the critical value 0.75 [15]. However, it is to be seen what happens for other classes of initial conditions. Here we want to cite an interesting study where both angles and velocities are initially distributed according to a function of the same form of that obtained at equilibrium, i.e., as in Eq. (5), but with the values of the parameters different from those at equilibrium [40]. The authors find that, depending on the values of the energy and of the initial magnetization, not only out-of-equilibrium stationary states can be realized, but also out-of-equilibrium periodic states are reached, in which the magnetization value oscillates. These results give their contribution to the evidence that, although a good deal of systematic studies have been performed on the HMF model, many issues still must be satisfactorily clarified.

ACKNOWLEDGMENTS

The present work has been supported by the PRIN05 grant on "Dynamics and thermodynamics of systems with long-range interactions". The authors thank S. Ruffo and A. Rapisarda for fruitful discussions.

APPENDIX A: THE DISTRIBUTION FUNCTIONS RELATED TO THE DIFFERENT CLASSES OF INITIAL CONDITIONS

We collect in this appendix the distributions describing the initial conditions studied in this paper. Let us denote with $\chi(x)$ the characteristic function of the segment $(-x,x)$, i.e., the function which is equal to 1 inside this segment and 0 otherwise. The distributions $f(\theta,p)=g(\theta)h(p)$ are the following. Except in the first case, where the initial magnetization m is equal to 1, and the third case, where it has a generic value, in the others it is equal to 0.

(i) Water bag (wb),

$$g(\theta)=\delta(\theta), \quad h(p)=\frac{1}{2p_{\mathrm{wb}}}\chi(p_{\mathrm{wb}}), \tag{A1}$$

with p_{wb} determined by the energy density ϵ by $p_{\mathrm{wb}}=\sqrt{6\epsilon}$.

(ii) Uniform (un),

$$g(\theta)=\frac{1}{2\pi}, \quad h(p)=\frac{1}{2p_{\mathrm{un}}}\chi(p_{\mathrm{un}}), \tag{A2}$$

with p_{un} given by $p_{\mathrm{un}}=\sqrt{6\left(\epsilon-\frac{1}{2}\right)}$; this case is possible if $\epsilon \geq 1/2$.

(iii) Partial magnetized (pm),

$$g(\theta)=\frac{1}{2\theta_m}\chi(\theta_m), \quad h(p)=\frac{1}{2p_{\mathrm{pm}}}\chi(p_{\mathrm{pm}}), \tag{A3}$$

with p_{pm} given by $p_{\mathrm{pm}}=\sqrt{6\left(\epsilon-\frac{1}{2}+\frac{1}{2}m^2\right)}$, and θ_m by the solution of the equation $[\sin(\theta_m)/\theta_m]=m$; this case is possible, for a given value of m, if $\epsilon \geq 1/2-m^2/2$.

(iv) Triangular (tr),

$$g(\theta)=\frac{1}{2\pi}, \quad h(p)=\left(b-\frac{b-a}{p_{\mathrm{tr}}}|p|\right)\chi(p_{\mathrm{tr}}), \tag{A4}$$

where the parameters p_{tr}, a, and $b \geq a$ satisfy the two relations $(b+a)p_{\mathrm{tr}}=1$ and $(b+3a)p_{\mathrm{tr}}^3=12\left(\epsilon-\frac{1}{2}\right)$; this case is possible if $\epsilon \geq 1/2$. Differently from the other cases considered in this work, at a given energy ϵ there remains a free parameter. The form of the distribution function $h(p)$ is that of a box surmounted by a triangle.

(v) Semielliptical (el),

$$g(\theta)=\frac{1}{2\pi}, \quad h(p)=\frac{2}{\pi p_{\mathrm{el}}}\sqrt{1-\frac{p^2}{p_{\mathrm{el}}^2}}\chi(p_{\mathrm{el}}), \tag{A5}$$

with p_{el} given by $p_{\mathrm{el}}=\sqrt{8\left(\epsilon-\frac{1}{2}\right)}$; this case is possible again if $\epsilon \geq 1/2$.

We have also considered (wb) initial conditions where the corresponding function $h(p)$ is not realized through the usual random number generations, but the N initial velocities are given by the values $p_i=-p_{\mathrm{wb}}+2p_{\mathrm{wb}}(i-1/2)/N$, $i=1,2,\ldots,N$. This special initial condition has been called (iwb). Loosely speaking, for $N\to\infty$ any realization of the (wb) should tend to (iwb).

APPENDIX B: THE STABILITY OF THE ELLIPTIC VELOCITY DISTRIBUTION FUNCTION AS A STATIONARY SOLUTION OF THE VLASOV EQUATION

The Vlasov equation for the one-particle distribution function $f(\theta,p,t)$ of the HMF system is given by [15,31]

$$\frac{\partial f}{\partial t}+p\frac{\partial f}{\partial \theta}-\frac{\partial U}{\partial \theta}\frac{\partial f}{\partial p}=0, \tag{B1}$$

where U is actually a function of (θ,t) and a functional of f given by

$$U=-\int d\alpha dp\, \cos(\theta-\alpha)f(\alpha,p,t). \tag{B2}$$

It is immediate to see that any distribution function which is homogeneous in θ, i.e., any distribution of the form $f(\theta,p)=h(p)/(2\pi)$, is a stationary solution of the Vlasov equation.

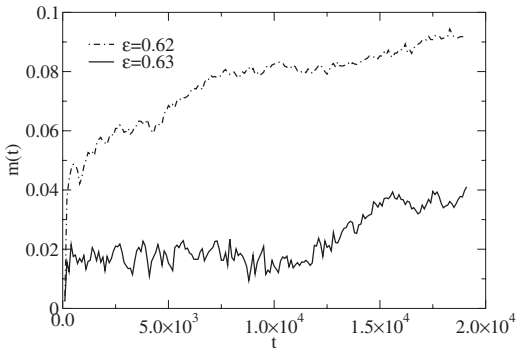

FIG. 13. Stability of the elliptic distribution. These simulations are for $N=262\,144$, (el) initial conditions, and two energy densities. Note that $\epsilon=0.62$ is below the stability threshold 0.625 and there is no stationary state.

The necessary condition for its stability can be expressed using the normalized distribution $h(p)$; the condition is [15,31]

$$1 + \frac{1}{2}\int_{-\infty}^{+\infty} \frac{h'(p)}{p} dp \geq 0. \tag{B3}$$

In the case of the (el) initial conditions, from the expression for $h(p)$ given in Appendix A we obtain

$$1 - \frac{1}{\pi p_{\mathrm{el}}^3}\int_{-p_{\mathrm{el}}}^{p_{\mathrm{el}}} \frac{dp}{\sqrt{1-\left(\frac{p}{p_{\mathrm{el}}}\right)^2}} \geq 0, \tag{B4}$$

that, after integration, gives: $1-\frac{1}{p_0^2} \geq 0$. Using the relation between p_{el} and ϵ given in Appendix A, we obtain that stability requires $\epsilon \geq \frac{5}{8} = 0.625$. Therefore the elliptic velocity distribution function is unstable if the energy density is below 0.625. Figure 13 numerically confirms, in a concrete case, this fact.

[1] T. Padmanabhan, Phys. Rep. **188**, 285 (1990).
[2] D. C. Brydges and P. A. Martin, J. Stat. Phys. **96**, 1163 (1999).
[3] D. H. E. Dubin and T. M. O'Neil, Rev. Mod. Phys. **71**, 87 (1999).
[4] Y. Elskens and D. F. Escande, *Microscopic Dynamics of Plasmas and Chaos* (IOP, Bristol, 2002).
[5] P. H. Chavanis, P. Sommeria, and R. Robert, Astrophys. J. **471**, 385 (1996).
[6] L. Q. English, M. Sato, and A. J. Sievers, Phys. Rev. B **67**, 024403 (2003).
[7] T. Dauxois, S. Ruffo, E. Arimondo, and M. Wilkens, *Dynamics and Thermodynamics of Systems with Long Range Interactions*, Lecture Notes in Physics, Vol. 602 (Springer, Berlin, 2002).
[8] R. S. Ellis, K. Haven, and B. Turkington, J. Stat. Phys. **101**, 999 (2000).
[9] F. Borgonovi, G. L. Celardo, M. Maianti, and E. Pedersoli, J. Stat. Phys. **116**, 1435 (2004).
[10] D. Mukamel, S. Ruffo, and N. Schreiber, Phys. Rev. Lett. **95**, 240604 (2005).
[11] M. Antoni and S. Ruffo, Phys. Rev. E **52**, 2361 (1995).
[12] J. Barré, T. Dauxois, G. De Ninno, D. Fanelli, and S. Ruffo, Phys. Rev. E **69**, 045501(R) (2004).
[13] M. Kac, G. E. Uhlenbeck, and P. C. Hemmer, J. Math. Phys. **4**, 216 (1963).
[14] J. Barré, F. Bouchet, T. Dauxois, and S. Ruffo, J. Stat. Phys. **119**, 677 (2005).
[15] Y. Y. Yamaguchi, J. Barré, F. Bouchet, T. Dauxois, and S. Ruffo, Physica A **337**, 36 (2004).
[16] V. Latora, A. Rapisarda, and C. Tsallis, Phys. Rev. E **64**, 056134 (2001).
[17] V. Latora, A. Rapisarda, and C. Tsallis, Physica A **305**, 129 (2002).
[18] C. Tsallis, J. Stat. Phys. **52**, 479 (1988).
[19] F. Bouchet and T. Dauxois, Phys. Rev. E **72**, 045103(R) (2005).
[20] A. Pluchino, V. Latora, and A. Rapisarda, Physica D **193**, 315 (2004).
[21] A. Rapisarda and A. Pluchino, Europhys. News **36**, 202 (2005).
[22] A. Campa, A. Giansanti, and D. Moroni, J. Phys. A **36**, 6897 (2003).
[23] W. Braun and K. Hepp, Commun. Math. Phys. **56**, 125 (1977).
[24] P. H. Chavanis, Eur. Phys. J. B **53**, 487 (2006).
[25] A. Antoniazzi, D. Fanelli, J. Barré, P. H. Chavanis, T. Dauxois, and S. Ruffo, Phys. Rev. E **75**, 011112 (2007).
[26] D. Lynden-Bell, Mon. Not. R. Astron. Soc. **136**, 101 (1967).
[27] H. Yoshida, Phys. Lett. A **150**, 262 (1990).
[28] A. Pluchino, V. Latora, and A. Rapisarda, Physica A **338**, 60 (2004).
[29] L. G. Moyano, F. Baldovin, and C. Tsallis, e-print arXiv:cond-mat/0305091.
[30] It should be noted that the symmetry of the equations of motion would imply that with the (iwb) initial conditions the y component of the magnetization m should rigorously remain fixed at 0; however, roundoff errors in the numerical simulations do not allow this conservation.
[31] S. Inagaki and T. Konishi, Publ. Astron. Soc. Jpn. **45**, 733 (1993).
[32] T. Padmanabhan, Astrophys. J., Suppl. Ser. **71**, 651 (1989).
[33] P. H. Chavanis, Astron. Astrophys. **381**, 340 (2002).
[34] P. H. Chavanis, Astron. Astrophys. **432**, 117 (2005).
[35] A. Campa, A. Giansanti, D. Mukamel, and S. Ruffo, Physica A **365**, 120 (2006).
[36] I. Ispolatov and M. Karttunen, Phys. Rev. E **68**, 036117 (2003).
[37] I. Ispolatov and M. Karttunen, Phys. Rev. E **70**, 026102 (2004).
[38] Actually, the entropy functional is a conserved quantity of the Vlasov equation, and therefore the Vlasov dynamics cannot change its value from the initial one; in particular, the functional will not be maximized by the dynamics. However, due to the mixing property of the dynamics, the functional will be maximized by any coarse-grained distribution, i.e., by the physically observable distribution.
[39] F. Bouchet and T. Dauxois, Phys. Rev. E **72**, 045103(R) (2005).
[40] H. Morita and K. Kaneko, Phys. Rev. Lett. **96**, 050602 (2006).